Check for updates

RESEARCH ARTICLE

Adsorption selectivity of water-ethanol mixtures on organosilica surfaces: Role of hydrophilicity

[version 1; peer review: 2 approved with reservations]

Simon Gravelle[1], Benoit Coasne[1,2]

[1]Univ. Grenoble Alpes, CNRS, LIPhy, 38000, Grenoble, France
[2]Institut Laue Langevin, F-38042 Grenoble, France

v1 **First published:** 09 Jun 2025, **5**:158
https://doi.org/10.12688/openreseurope.19509.1
Latest published: 09 Jun 2025, **5**:158
https://doi.org/10.12688/openreseurope.19509.1

Abstract

Background

The competition between hydrophilic and hydrophobic interactions in water-ethanol mixtures gives rise to abnormal properties, such as the formation of an ethanol-rich surface layer at non-polar interfaces like graphite. This phenomenon, resulting from the balance between solid-liquid and liquid-liquid interactions, could benefit the development of microporous membranes for separating water-alcohol mixtures.

Methods

We used molecular dynamics simulations of water-ethanol mixtures near planar organosilica surfaces, focussing on the role of surface properties in interfacial ethanol enrichment. Surface hydrophobicity was controlled by adjusting the ratio of methyl to hydroxyl groups. We analyzed the impact of surface composition, roughness, and the spatial distribution of functional groups on ethanol adsorption.

Results

Our simulations reveal that ethanol preferentially adsorbs onto hydrophobic organosilica surfaces functionalized with methyl groups, similar to previous findings for graphite. Ethanol enrichment is strongly influenced by mixture composition and surface properties, including roughness and functional group distribution. Hydrophobic surfaces consistently exhibit enhanced ethanol affinity, whereas hydroxylated surfaces show weaker adsorption.

Open Peer Review

Approval Status ? ?

	1	2
version 1 09 Jun 2025	? view	? view

1. **Aziz Ghoufi**, Paris-East Créteil University, Créteil, France

2. **Eric Breynaert**, NMRCoRe—NMR/X-Ray Platform for Convergence Research, Heverlee, Belgium

Any reports and responses or comments on the article can be found at the end of the article.

Conclusions

These findings demonstrate the ability of organosilica materials to preferentially adsorb ethanol over water. Overall, this work identifies a cost-effective alternative to carbon-based materials for the fabrication of filtration membranes.

Keywords
molecular dynamics, filtration, water, ethanol, organosilica, adsorption



This article is included in the Marie-Sklodowska-Curie Actions (MSCA) gateway.



This article is included in the Horizon Europe gateway.

Corresponding author: Simon Gravelle (simon.gravelle@cnrs.fr)

Author roles: Gravelle S: Conceptualization, Funding Acquisition, Investigation, Writing – Original Draft Preparation, Writing – Review & Editing; **Coasne B**: Conceptualization, Investigation, Supervision, Writing – Review & Editing

Competing interests: No competing interests were disclosed.

Grant information: This project has received funding from the European Union's Horizon 2020 research and innovation programme under the Marie Sklodowska-Curie grant agreement N ◦ 101065060. Most of the computations presented in this paper were performed using the GRICAD infrastructure (https://gricad.univ-grenoble-alpes.fr), which is supported by Grenoble research communities. In addition, this work was granted access to the HPC resources of IDRIS under the allocation 2023-AD012A14560 made by GENCI.

Copyright: © 2025 Gravelle S and Coasne B. This is an open access article distributed under the terms of the Creative Commons Attribution License, which permits unrestricted use, distribution, and reproduction in any medium, provided the original work is properly cited.

How to cite this article: Gravelle S and Coasne B. **Adsorption selectivity of water-ethanol mixtures on organosilica surfaces: Role of hydrophilicity [version 1; peer review: 2 approved with reservations]** Open Research Europe 2025, **5**:158 https://doi.org/10.12688/openreseurope.19509.1

First published: 09 Jun 2025, **5**:158 https://doi.org/10.12688/openreseurope.19509.1

Introduction

Ethanol is a widely used biofuel that provides a lower-emission alternative to gasoline[1]. Biofuels are produced from the fermentation of crops, a process that yields a mixture of water and ethanol. To obtain high-purity ethanol for use as fuel, the mixture must be separated. The separation of water-ethanol mixtures is typically done using distillation-based methods that require heat and high pressures, resulting in significant energy consumption[2]. In response to this challenge, ongoing efforts are aimed at developing more efficient separation technologies, such as isothermal filtration with microporous membranes[3].

Binary mixtures like water-ethanol have been the focus of intensive research since the pioneering work by Frank and Evans in 1945[4]. Yet, the properties of such mixtures are still under active investigation due to the complex nature of their interactions[5]. Ethanol is a weakly amphiphilic molecule with a hydrophilic head and a non-polar tail. When mixed with water, it exhibits numerous anomalous behaviors compared to pure solvents. For instance, the hydrophobic segments of ethanol tend to cluster together to avoid interaction with water, while the hydrophilic heads form polar interactions with water[6]. The competition between hydrophilic and hydrophobic interactions gives rise to several anomalies, such as incomplete mixing of water and alcohol, local microheterogeneity, and a negative excess entropy[7].

When a water-ethanol mixture is in contact with an interface, an equilibrium configuration that best satisfies the competition between entropy and enthalpy is established. Next to non-polar solids such as graphene or hexagonal boron nitride, ethanol and other alcools tend to accumulate over water within the first density layer[8–13]. A similar surface accumulation of ethanol occurs at liquid-vapor interfaces, where the surface ethanol molar fraction can exceed the bulk molar fraction by a factor that depends, among other factors, on the mixture composition[14,15]. Conversely, polar interfaces like hydrophilic silica surfaces show little to no preference for ethanol adsorption over water[16,17], while polar alumina surfaces exhibit a preference for water adsorption over ethanol[18,19].

The molecular enrichment of ethanol over water at non-polar interfaces could form the basis for microporous membrane separation. To achieve effective large-scale separation, membranes must feature well-controlled hierarchical porosity, strong mechanical properties to with stand the high pressures involved in separation processes, and must also be cost-effective and durable[20–23]. Fabricating membranes based on graphene or its derivatives, such as carbon nanotubes, is currently impractical[24], but a promising alternative is nanoporous organosilica[25,26]. Organosilica materials are composed of nanoporous silica functionalized with organic compounds, such as methyl groups or hydrocarbons[16,27]. Organosilica membranes combine excellent mechanical properties with tunable hydrophobic/hydrophilic surfaces[28,29], making them a compelling candidate for fluid separation applications.

In this study, the properties of water-ethanol mixtures near organosilica surfaces with varying functionalizations and structures are examined using molecular dynamics simulations. The organosilica surfaces are functionalized with a fraction $r_{C/O}$ of non-polar ($-CH_3$) groups and a fraction $1 - r_{C/O}$ of polar ($-OH$) groups. By exploring a wide range of $r_{C/O}$ values (from 0 to 1), we create surfaces with a broad spectrum of hydrophilicities. The composition and structure of the fluid near these surfaces are analyzed and compared with those near a graphite surface and a liquid-vapor interface.

Methods

Molecular dynamics simulations of a mixture of water and ethanol in a silica-based slit pore were performed using GROMACS[30]. The composition of the mixture was varied from $x^{eth}_{total} = 0$ (pure water) to $x^{eth}_{total} = 1$ (pure ethanol), where

$$x^{eth}_{total} = \frac{N^{eth}}{N^{eth} + N^{wat}}, \quad (1)$$

is the total ethanol number fraction, with N^{eth} and N^{wat} representing the numbers of ethanol and water molecules in the simulation. In most of the simulations presented here, the mixture contained 150 ethanol molecules and 2850 water molecules, corresponding to an ethanol number fraction $x^{eth}_{total} = 0.05$ and a mass $r^{eth}_{total} = 0.12$. For each simulation, the ethanol mass fraction in the bulk (i.e., far from the surfaces), r^{eth}_{bulk}, was measured after the equilibrium was established. Generally, r^{eth}_{bulk} differs from r^{eth}_{total} due to the preferential surface adsorption of one species over the other, as illustrated, for example, in Figure 1A.

Unless stated otherwise, the surfaces of the slit pores were constructed from a Q^3 silica material characterized by a surface group density of 5 nm^{-2} (Figure 1). Here, the index '3' in Q^3 refers to the number of bridging oxygens connected to a silicon atom. The dangling Si atoms of the silica were functionalized with non-polar (-CH_3) groups at a fraction $r_{C/O}$ and polar (-OH) groups at a fraction $1 - r_{C/O}$. Slit pores made from Q^2 silica, mixed Q^2/Q^3 silica, mixed Q^3/Q^4 silica, Q^4 silica, amorphous silica, and graphite were also generated (Figure 1). For comparison, simulations of a liquid-vapor interface were also carried out. For $r_{C/O} = 0$, the Q^3 solid surface is hydrophilic, exhibiting a measured water contact angle of approximately 40° (Fig. S1). In contrast, for $r_{C/O} = 1$, the surface is hydrophobic, with a measured water contact angle of approximately 90°[31,32].

The distance between the two walls of the slit pore, h, was approximately 8 nm, while the system dimensions along the x and y axes were approximately 3 nm (Figure 1). The system was first equilibrated at ambient temperature ($T = 300$ K) and pressure ($p = 1$ atm) for a total duration of 50 ns, allowing the density profile to stabilize. During this equilibration step, the temperature was maintained using the Canonical Sampling through Velocity Rescaling (CSVR) thermostat[33] with a time constant of 0.1 ps, and the pressure was maintained using an anisotropic Berendsen barostat[34] with a time constant of 1 ps. Water was modeled with the TIP4P/ϵ model[35], and ethanol was modeled using the OPLS/AA force field[36]. Cross parameters were calculated using the Lorentz-Berthelot mixing

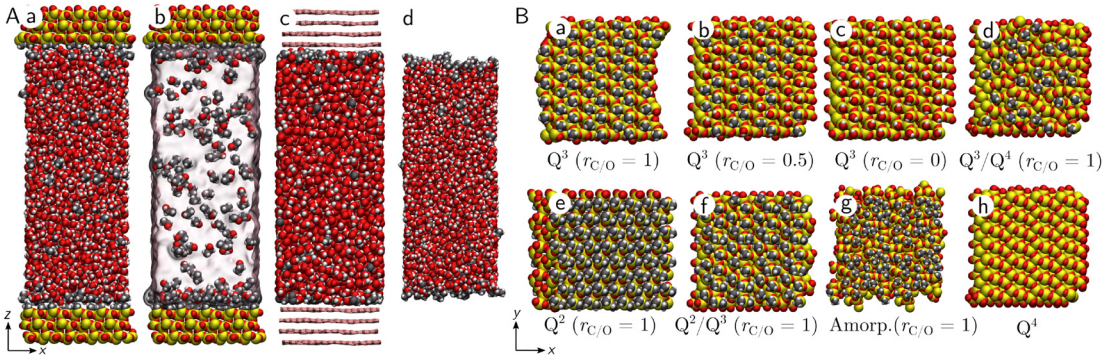

Figure 1. (**A**) Side view of a water-ethanol mixture with x^{eth}_{total} = 0.05 confined inside an organosilica slit pore with $r_{C/O}$ = 0 (a and b), a graphite pore (c), and two liquid-vapor interfaces (d). Oxygen atoms are represented in red, carbon atoms in gray, silicon in yellow, and hydrogen in white. In panel b, water is represented as a continuous transparent field for clarity, and in panel c, the carbon atoms of graphite are represented as pink bonds. (**B**) Top view of different silica surfaces considered here: Q^3 surface with $r_{C/O}$ = 1.0 (a), $r_{C/O}$ = 0.5 (b), and $r_{C/O}$ = 0.0 (c), Q^3/Q^4 surface with $r_{C/O}$ = 1.0 (d), Q^2 surface with $r_{C/O}$ = 1.0 (e), Q^3/Q^4 surface with $r_{C/O}$ = 1.0 (f), amorphous surface with $r_{C/O}$ = 1.0 (g), and Q^4 surface (h).

rule. The SURFACE force field was used for silica[37], along with the GROMOS force field, which was used for the $-CH_3$ groups[38]. The simulation scripts are available in a public online repository[39].

Results

Density profiles

First, density profiles normal to the solid surface were extracted for both water and ethanol, using the MAICoS toolkit[40] (Figure 2). Here, the fluid is mostly composed of water, with an ethanol mass fraction r^{eth}_{total} = 0.12. For one of the most hydrophobic silica surfaces considered here, where $r_{C/O}$ = 1, our results indicate ethanol accumulation within the first density layer next to the solid surface (blue line in Figure 2A). Our results also show that, when $r_{C/O}$ = 1, water is partially depleted from the first density layer (blue line in Figure 2B). By contrast, for a more hydrophilic silica surface with $r_{C/O}$ = 0, our results show an accumulation of both species within the first density layer (red lines in Figure 2A and B). Regardless of the surface hydrophilicity, there is a clear structuring of the fluid next to the solid interface, as indicated by the oscillations in the total fluid density $\rho^{tot} = \rho^{eth} + \rho^{wat}$ (Fig. S2). The maximum density value is approximately 0.75 u/Å^3 (about 25 % higher than in bulk) and is largely independent of the value of $r_{C/O}$.

For comparison, density profiles were also extracted for a graphite slit pore and a liquid-vapor interface. Both the graphite slit pore and the liquid-vapor interface show an accumulation of ethanol within the first density layer (dark lines in Figure 2), in good agreement with previous works[10,14,15]. In the case of graphite, the maximum fluid density within the first layer reaches a higher value compared to silica surfaces: 1.0 u/Å^3 (dark dashed line in Fig. S2). In contrast, silica reaches about 0.75 u/Å^3. Our results also show that the first layer of fluid next to a graphite surface is thinner than that next to a silica surface (dark dashed lines in Figure 2). In contrast, the first fluid layer at a liquid-vapor interface is broader than those at any of the solid surfaces considered here (dark dotted lines in Figure 2), highlighting differences in the fluid structuring that will be analyzed below.

Surface enrichment

To quantify the surface enrichment of ethanol over water at the interfaces, we measure the ethanol mass fraction within the first density layer, which we define as

$$r^{eth}_1 = \frac{\rho^{eth}_1}{\rho^{eth}_1 + \rho^{wat}_1}, \tag{2}$$

where the index '1' refers to the first fluid layer adjacent to the interface. The molecules of the first density layer were identified using the ITIM algorithm of Pytim[41,42] (see examples of the first four detected layers in Fig. S3). For comparison, the ethanol mass fraction was also measured in the bulk region, defined as the fluid molecules not belonging to the four detected layers (typically corresponding to molecules located at distances greater than approximately 1.2 nm from any interface):

$$r^{eth}_{bulk} = \frac{\rho^{eth}_{bulk}}{\rho^{eth}_{bulk} + \rho^{wat}_{bulk}}. \tag{3}$$

The ethanol enrichment factor was then defined as

$$E^{eth}_1 = \frac{r^{eth}_1}{r^{eth}_{bulk}}. \tag{4}$$

$E^{eth}_1 > 1$ indicates that ethanol is enriched in the first density layer relative to the bulk.

For the most hydrophobic organosilica surfaces considered here, and for an ethanol mass fraction r^{eth}_{total} = 0.12, the ethanol enrichment factor $\gtrapprox$ 10 (Figure 3A). The best-performing silica surface,for which $E^{eth}_1 \approx 13$, is the Q_2 silica surface with

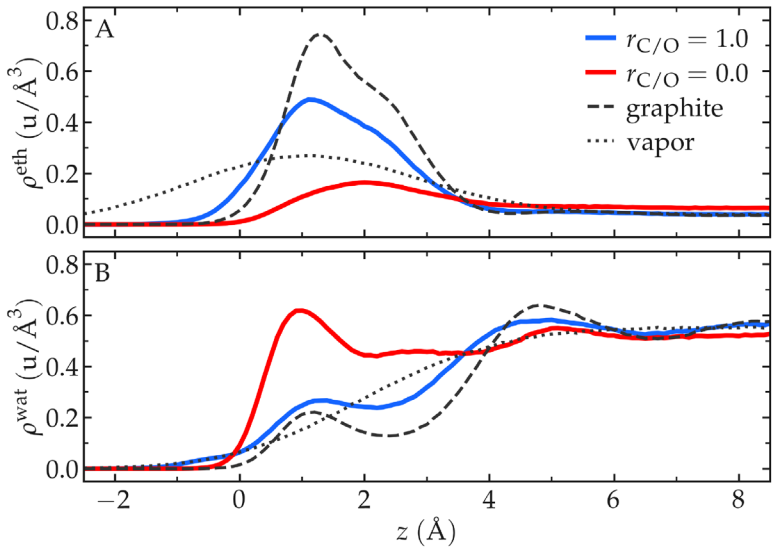

Figure 2. Density profiles next to the interface for ethanol, ρ^{eth}, (**A**) and water, ρ^{wat}, (**B**), respectively. The position z = 0 corresponds to the Gibbs dividing plane, and the bulk ethanol number fraction far from the solid surface is $r^{eth}_{bulk} \approx 0.05$. The results were obtained with Q^3 organosilica surfaces with two different values for the ratio $r_{C/O}$: $r_{C/O}$ = 1 corresponding to a hydrophobic surface (full blue line) and $r_{C/O}$ = 0 corresponding to a hydrophilic surface (full red line). The dashed dark line was obtained with graphite, and the dotted dark line with a liquid-vapor interface.

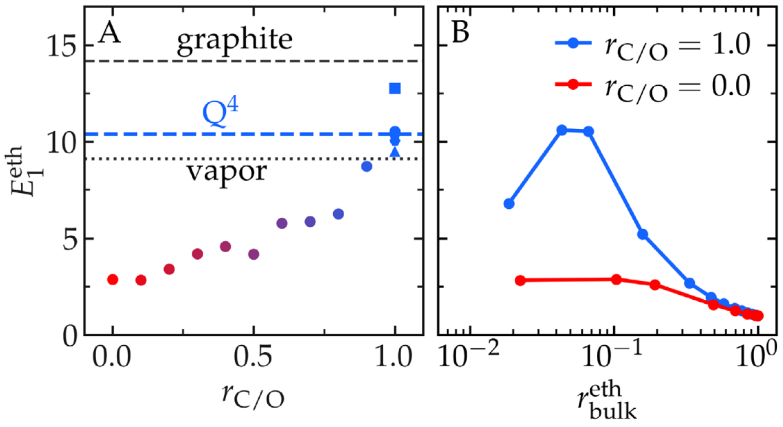

Figure 3. The ethanol enrichment factor, E_1^{eth} within the first density layer next to the interface [see Equation (4)]. **A**) E_1^{eth} as a function of the carbon-to-oxygen ratio, $r_{C/O}$, of the organosilica surfaces, from $r_{C/O}$ = 0 (hydrophilic surface) to $r_{C/O}$ = 1 (hydrophobic surface). The ethanol mass fraction is r^{eth}_{total} = 0.12. The dark dashed line is E_1^{eth} in the case of the graphite surface, the blue dashed line corresponds to the Q^4 surface, and the dark dotted line corresponds to the liquid-vapor interface. Disks are the default Q^3 surface, the square is Q^2, the pentagone is Q^2/Q^3, the hexagone is the amorphous surface, and the triangle is Q^3/Q^4. **B**) E_1^{eth} as a function of the bulk ethanol mass fraction, r^{eth}_{bulk} in the case of the hydrophobic surface with $r_{C/O}$ = 1 (blue), and hydrophilic surface with $r_{C/O}$ = 0 (red).

$r_{C/O}$ = 1. The Q_2 silica surface has the highest surface group density of all the organosilica structures considered here (Figure 1B), a property that will be discussed below. Interestingly, for the most hydrophilic surfaces considered here with $r_{C/O}$ = 0, the ethanol enrichment factor exceeds one ($E_1^{eth} \approx 3$) indicating preferential ethanol adsorption even on polar surfaces. By comparison, for graphite, $E_1^{eth} \approx 14$, slightly exceeding the best organosilica surfaces (dashed line in Figure 3A). At the liquid-vapor interface, $E_1^{eth} \approx 9$ which is lower than that of all organosilica surfaces with $r_{C/O}$ = 1 (dotted line in Figure 3A).

Results for the organosilica surfaces with $r_{C/O}$ = 1 and varying reservoir composition r^{eth}_{bulk} show a non-homogeneous variation in E_1^{eth}, with an optimum near r^{eth}_{bulk} = 0.05 (Figure 3B). In the case of reservoirs of pure ethanol (i.e., $r^{eth}_{bulk} \to 1$), $E_1^{eth} \to 1$ as expected. For reservoirs rich in water (i.e., $r^{eth}_{bulk} \to 0$), E_1^{eth} is

lower than when $r_{bulk}^{eth} \approx 0.05$, which reveals an enhancement of surface ethanol enrichment at intermediate concentrations. The origin of this enhancement could be the hydrophobic interactions between ethanol molecules, as will be discussed below. For the hydrophilic silica with $r_{C/O} = 0$, $E_1^{eth} \lessapprox 2.5$, regardless of the reservoir composition.

The ethanol enrichment factor was also calculated within the second density layer (i.e., E_2^{eth}) next to the solid surface (Fig. S4 A). Our results show that E_2^{eth} is nearly independent of $r_{C/O}$, suggesting that the surface properties mainly affect the fluid composition of the first density layer, with only a minor impact on the second density layer. However, with $E_2^{eth} \approx 1.1$, the second layer is slightly richer in ethanol than the bulk reservoir, implying that the surface influence extends beyond the first density layer, as also seen in the oscillations of the total density (Fig. S2). Our results also show that within the second layer and in the limit $r_{bulk}^{eth} \to 0$, E_2^{eth} is lower than 1, indicating a slight depletion in ethanol (Fig. S4 B).

The results in Figure 3A indicate that the ratio of polar to non-polar groups, $r_{C/O}$, is the primary factor determining ethanol enrichment at an organosilica surface. However, Figure 3A also demonstrates that $r_{C/O}$ is not the sole determinant, as surfaces with $r_{C/O} = 1$ exhibit a wide range of enrichment values, E_1^{eth} from approximately 9.5 (for the Q^3/Q^4 surface) to approximately 13 (for the Q^2 surface). This suggests that additional parameters, beyond $r_{C/O}$, influence ethanol enrichment. One likely candidate is the surface group density, characterized by the number of -CH_3 groups per unit surface area, n_{CH3}. This parameter ranges from 0 (Q^4 surface) to approximately 9nm^{-2} (Q^2 surface) (Figure 4A). Interestingly, the relationship between n_{CH3} and E_1^{eth} is non-monotonic, with relatively high ethanol enrichment observed at both small and large values of n_{CH3}. This observation indicates that other factors, alongside n_{CH3} and $r_{C/O}$, likely contribute to ethanol enrichment at the interface. These factors are further explored in the next section.

Surface -CH_3 patches

The results obtained with different types of silica surfaces (Figure 4A) indicate that while the number of surface groups, n_{CH3}, is a useful indicator of surface efficiency in separating ethanol and water, it does not fully account for the preferential adsorption of ethanol. Notably, the Q^4 surface achieves reasonable a value for E_1^{eth} despite having no surface groups. We hypothesize that surface atomic roughness and the specific organization of surface groups play significant roles in the ethanol enrichment (Figure 1B). To test this hypothesis, -CH_3 patches were defined as the largest possible ellipses connecting neighboring $-CH_3$ groups within the (x, y) plane

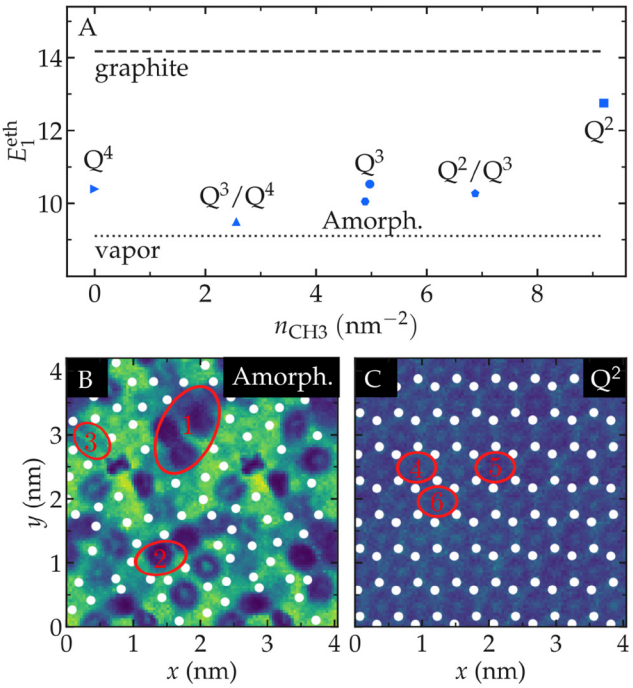

Figure 4. A) Ethanol enrichment factor within the first density layer, E_1^{eth} as a function of the surface density of CH_3 groups, n_{CH3}, for the six organosilica surfaces considered: Q^4, Q^3, Q^2, Q^3/Q^4, Q^2/Q^3, and amorphous. The dashed line represents E_1^{eth} for graphite, and the dotted line corresponds to the liquid-vapor interface. **B**–**C**) Density maps of the ethanol mass fraction within the first density layer, r_1^{eth} for the amorphous and Q_2 organosilica surfaces with $r_{C/O} = 1$. Yellow indicates a low ethanol fraction ($r_1^{eth} = 0$), while blue indicates a high ethanol fraction ($r_1^{eth} = 1$). White dots mark the average positions of the $-CH_3$ groups. In panel B, red ellipses highlight a large patch (n◦1) with surface area $A_p \approx 1$ nm^2, and two medium-sized patches (n◦2 with $A_p \approx 0.33$ nm^2 and n◦3 with $A_p \approx 0.28$ nm^2). In panel C, all patches are of similar size ($A_p \approx 0.23$ nm^2).

(red ellipses in Figure 4B, C). We found that the most heterogeneous surfaces considered here, such as amorphous and Q^3/Q^4, exhibit $-CH_3$ patches with surface areas as large as $A_p \approx 1nm^2$, alongside smaller patches with $A_p \approx 0.3nm^2$. In contrast, more regular surfaces, like Q^2, show only smaller patches ranging in size from 0.2 to $0.3nm^2$ (Figure 4B, C and Fig. S5).

The ethanol mass fraction, r_1^{eth}, was measured within individual patches (Fig. S6). Although no clear relationship between patch size and local ethanol enrichment could be established, certain trends emerged. Large patches with $A_p > 0.4nm^2$ consistently exhibit high fraction r_1^{eth}, which aligns with the high E_1^{eth} value observed for the Q^4 surface despite its lack of surface groups. Conversely, all patches with low ethanol fraction (i.e., $r_1^{eth} < 0.8$) fall within the size range of $0.1nm^2 < A_p < 0.3nm^2$. However, many patches within this range, including all patches from the Q^2 and Q^3 surfaces, exhibit high ethanol fraction (see for example patches n°2 and n°3 in Figure 4B). These findings suggest that while patch size may play a role in local ethanol enrichment, a more detailed characterization of the atomic structure is required. Such characterization could involve surface topography (e.g. positions of $-CH_3$ groups along the z axis normal to the surface) and/or the distribution of local surface dipole moments.

Hydrogen bonding

To further caracterize the state of water-ethanol mixtures within the first layers next to the solid surfaces, the number of OH· · · O hydrogen bonds per molecule, n_{HB}, was measured[31]. Our results indicate that for a fixed reservoir composition ($r_{total}^{eth} = 0.12$), the number of hydrogen bonds per ethanol molecule in the first density layer decreases with the enrichment factor E_1^{eth} (Figure 5 A)[43]. On surfaces with low E_1^{eth} (i.e., hydrophilic surfaces), the number of hydrogen bonds per ethanol molecule is approximately 2, similar to what is measured in bulk. However, on surfaces with high E_1^{eth}, this number decreases to 1.75. A qualitatively similar trend is observed for water, for which n_{HB} decreases from approximately 3.1 to 2.6 as E_1^{eth} increases. This reduction can be partially attributed to the absence of hydrogen bonds between molecules and non-polar surface groups (Fig. S7).

Results from Figure 5A indicate that for both water and ethanol, adsorbing at non-polar surfaces implicate a reduction in the number of hydrogen bonds compared to the bulk. That reduction is however slightly larger for water (about 16 %) than for ethanol (about 12 %). In addition to the value of n_{HB}, there is a well known advantage associated with concentrating the ethanol molecules at the interfaces: it mitigates the disturbance to the hydrogen bond network in the fluid by allowing water molecules to form more hydrogen bonds with themselves[7,44]. To caracterise this effect, we counted the number of neighboring ethanol carbon-carbon atoms, $N_{C\text{-}C}$. Our results show that, for low E_1^{eth} (i.e., hydrophilic surfaces), $N_{C\text{-}C} \approx 0.75$ for both ethanol molecules from the bulk and the first density layer (Figure 5B). This indicates that in the case of the most hydrophilic surfaces, there is no visible clustering of ethanol molecules within the first density layer. As E_1^{eth} increases, $N_{C\text{-}C}$ from the first density layer increases up to almost 2, while $N_{C\text{-}C}$ from the bulk decreases below 0.5. Interestingly, all data points in Figure 5B fall on the same master curve, except for the vapor interface and the amorphous silica surface, for which $N_{C\text{-}C}$ is lower, suggesting that the specifity of the interface can favor or hinder the contact between ethanol carbon-carbon atoms, with possible impact on the selective adsorption.

Discussion

Our results for varying reservoir composition reveal a maximum in the ethanol enrichment at an ethanol mass fraction of $r_{bulk}^{eth} = 0.05$, in the case of organosilica surfaces with $r_{C/O} = 1$ (Figure 3B). This suggests that collective effects may enhance surface enrichment. One likely contributor is the hydrophobic interaction between clustering ethanol molecules[5,45], an effect that is expected to only be significant at intermediate ethanol concentrations and to diminish as $r_{bulk}^{eth} \to 0$. Indeed, the typical number of neighboring ethanol carbon-carbon atoms, $N_{C\text{-}C}$,

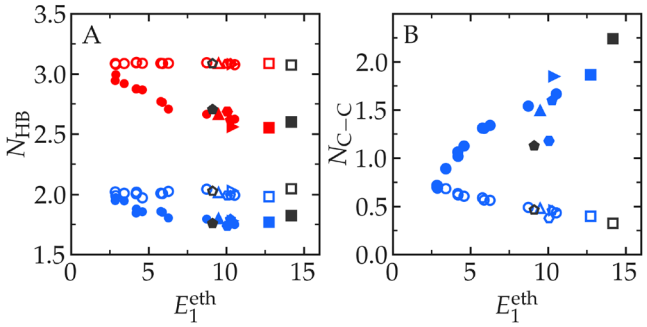

Figure 5. A) Number of OH· · · O hydrogen bonds, N_{HB}, per ethanol (blue) and water (red) molecule as a function of the enrichment factor E_1^{eth}. Filled symbols represent measurements from the first density layer, while open symbols are from the bulk. Symbols correspond to different surfaces: disks for Q^3, squares for Q^2, pentagons for Q^2/Q^3, hexagons for amorphous, upward triangles for Q^3/Q^4, and rightward triangles for Q^4. The gray pentagones are results from the vapor interface, and the gray squares are from graphite. The ethanol mass fraction is $r_{total}^{eth} = 0.12$. **B**) Number of neighboring carbon atoms per carbon atom, $N_{C\text{-}C}$, from ethanol molecules in the first density layer (filled symbols) and in the bulk (open symbols) as a function of E_1^{eth}. Only carbon atoms located within a distance $r < 4.6$ Å and from different molecules are considered, see Ref. 31.

shows an inflection point near $r_{bulk}^{eth} \approx 0.1$ (Figs. S8-S9). This indicates that, below r_{bulk}^{eth}, there is a substantial decrease in ethanol-ethanol hydrophobic interactions within the first layer. Such a decrease aligns with the observed reduction in ethanol enrichment as $r_{bulk}^{eth} \to 0$. These findings suggest that membrane separation based on the preferential adsorption of ethanol over water could lose efficiency in the limit of vanishing ethanol concentrations.

The surfaces considered in this study exhibit varying degree of atomic roughness, ranging from the atomically smooth graphite to the disordered amorphous silica surface (Figure 1). These differences in surface roughness lead to distinct structuring of molecules within the first density layer, as revealed by 1D (Figure 2) and 2D (Figure 4) density profiles, the number of neighboring ethanol carbon-carbon atoms $N_{C\text{-}C}$ (Figure 5B), as well as orientation distribution of molecules within the first layer (Fig. S10). However, despite these differences, certain generic trends emerge across all surfaces. For example, the number of hydrogen bonds per molecule, n_{HB}, from all systems follows the same master curves (Figure 5A). Additionally, the thickness of the first density layer, σ_1, measured as the variance of the density profile $\rho_1(z)$ [see Eq. (S2)], decreases with increasing ethanol enrichment factor, E_1^{eth} (Fig. S11). In other words, surfaces with thinner first density layer tend to exhibit better ethanol-water separation performance.

Although our results show that silica surfaces decorated with $-CH_3$ are not as effective as pristine graphite for selectively adsorbing ethanol over water, they also reveal that even the least effective surfaces considered here (i.e., the Q^2/Q^3 and amorphous surfaces) show an ethanol enrichment factor of about 10 for $r_{total}^{eth} = 0.12$. This indicates that the enrichment of ethanol at hydrophobic silica surfaces is quite robust and should be measurable with any nanoporous silica-based material primarily decorated with non-polar groups, regardless of its structure.

Conclusion

In conclusion, we used molecular simulations to study the preferential adsorption of ethanol over water at organosilica surfaces. Our results reveal that the primary predictors of an organosilica surface ability to separate ethanol from water are the type and density of surface groups. The organosilica surface exhibiting the highest ethanol enrichment is a Q^2 surface fully decorated with non-polar groups ($r_{C/O} = 1$). This surface features a high density of $-CH_3$ groups ($n_{CH3} \approx 9 nm^{-2}$), and performs nearly as well as pristine graphite in preferentially adsorbing ethanol over water. Our study also highlights the non-trivial influence of surface atomic structure on ethanol enrichment. Surfaces with disordered groups, such as amorphous and Q^2/Q^3 surfaces, exhibit the poorest performance. This reduced enrichment could arise from geometric effects, as smaller water molecules may more readily adapt to rough landscapes (thereby decreasing ethanol enrichment), or from an increased local polarity associated with disordered surfaces.

Data availability

Underlying data

Zenodo: Underlying data for 'Adsorption selectivity of water-ethanol mixtures on organosilica surfaces: Role of hydrophilicity', https://doi.org/10.5281/zenodo.14961713[39].

Data are available under the terms of the Creative Commons Attribution 4.0 International license (CC-BY 4.0) (https://creativecommons.org/licenses/by/4.0/).

Software availability

Source code available from GitHub, under the https://github.com/simongravelle/publication-data[39].

Archived software available from: https://doi.org/10.5281/zenodo.14961713[39]

License: CC-BY 4.0

References

1. IEA Renewables: **Catalysing energy technology transformations.** 2019.
Reference Source
2. Semiat R: **Energy issues in desalination processes.** *Environ Sci Technol.* 2008; **42**(22): 8193–8201.
PubMed Abstract | **Publisher Full Text**
3. Belfort G: **Membrane filtration with liquids: a global approach with prior successes, new developments and unresolved challenges.** *Angew Chem Int Ed Engl.* 2019; **58**(7): 1892–1902.
PubMed Abstract | **Publisher Full Text**
4. Frank HS, Evans MW: **Free volume and entropy in condensed systems III. Entropy in binary liquid mixtures; Partial molal entropy in dilute solutions; structure and thermodynamics in aqueous electrolytes.** *J Chem Phys.* 1945; **13**: 507–532.
Publisher Full Text
5. Požar M, Lovrinčević B, Zoranić L, *et al.*: **Micro-heterogeneity *versus* clustering in binary mixtures of ethanol with water or alkanes.** *Phys Chem Chem Phys.* 2016; **18**(34): 23971–23979.
PubMed Abstract | **Publisher Full Text**
6. González-Salgado D, Nezbeda I: **Excess properties of aqueous mixtures of methanol: simulation versus experiment.** *Fluid Phase Equilib.* 2006; **240**(2): 161–166.
Publisher Full Text
7. Dixit S, Crain J, Poon WCK, *et al.*: **Molecular segregation observed in a concentrated alcohol-water solution.** *Nature.* 2002; **416**(6883): 829–832.
PubMed Abstract | **Publisher Full Text**
8. Gravelle S, Yoshida H, Joly L, *et al.*: **Carbon membranes for efficient water-ethanol separation.** *J Chem Phys.* 2016; **145**(12): 124708.
PubMed Abstract | **Publisher Full Text**
9. Gao Q, Zhu Y, Ruan Y, *et al.*: **Effect of adsorbed alcohol layers on the behavior of water molecules confined in a graphene nanoslit: a molecular dynamics study.** *Langmuir.* 2017; **33**(42): 11467–11474.
PubMed Abstract | **Publisher Full Text**
10. Kommu A, Singh JK: **Separation of ethanol and water using graphene and hexagonal boron nitride slit pores: a molecular dynamics study.** *J Phys Chem C.* 2017; **121**(14): 7867–7880.
Publisher Full Text

11. Metya AK: **Insight into the structure and dynamics of ethanol-water binary mixture confined in nanochannel by mica and graphene.** *J Phys Chem B.* 2022; **126**(38): 7385–7392.
PubMed Abstract | Publisher Full Text

12. Bellido-Peralta R, Leoni F, Calero C, *et al.*: **Exploring optimal graphene Slit-Pore width for the physical separation of water-methanol mixture.** *J Mol Liq.* 2023; **391**(Part B): 123356.
Publisher Full Text

13. Essafri I, Artzner F, Ghoufi A: **Nanoscale surface tension, adsorption isotherms and separation of water-ethanol mixtures confined between graphene-based Slit Pores.** *J Phys Chem C.* 2024; **128**(38): 16208–16219.
Publisher Full Text

14. Wilson MA, Pohorille A: **Adsorption and solvation of ethanol at the water liquid-vapor interface: a molecular dynamics study.** *J Phys Chem B.* 1997; **101**(16): 3130–3135.
PubMed Abstract | Publisher Full Text

15. Stewart E, Shields RL, Taylor RS: **Molecular dynamics simulations of the liquid/vapor interface of aqueous ethanol solutions as a function of concentration.** *J Phys Chem B.* 2003; **107**(10): 2333–2343.
Publisher Full Text

16. Guo XY, Watermann T, Sebastiani D: **Local microphase separation of a binary liquid under nanoscale confinement.** *J Phys Chem B.* 2014; **118**(34): 10207–10213.
PubMed Abstract | Publisher Full Text

17. Muthulakshmi T, Dutta D, Maheshwari P, *et al.*: **Evidence for confinement induced phase separation in ethanol-water mixture: a positron annihilation study.** *J Phys Condens Matter.* 2017; **30**(2): 025001.
PubMed Abstract | Publisher Full Text

18. Rao MB, Sircar S: **Liquid-phase adsorption of bulk ethanol-water mixtures by alumina.** *Adsorp Sci Technol.* 1993; **10**(1–4)**: 93–104.**
Publisher Full Text

19. Phan A, Cole DR, Striolo A: **Preferential adsorption from liquid water-ethanol mixtures in alumina pores.** *Langmuir.* 2014; **30**(27): 8066–8077.
PubMed Abstract | Publisher Full Text

20. Elimelech M, Phillip WA: **The future of seawater desalination: energy, technology, and the environment.** *Science.* 2011; **333**(6043): 712–717.
PubMed Abstract | Publisher Full Text

21. Sholl DS, Lively RP: **Seven chemical separations to change the world.** *Nature.* 2016; **532**(7600): 435–437.
PubMed Abstract | Publisher Full Text

22. Coasne B: **Multiscale adsorption and transport in hierarchical porous materials.** *New J Chem.* 2016; **40**(5): 4078–4094.
Publisher Full Text

23. Park HB, Kamcev J, Robeson LM, *et al.*: **Maximizing the right stuff: the trade-off between membrane permeability and selectivity.** *Science.* 2017; **356**(6343): eaab0530.
PubMed Abstract | Publisher Full Text

24. Liu G, Jin W, Xu N: **Graphene-based membranes.** *Chem Soc Rev.* 2015; **44**(15): 5016–5030.
Publisher Full Text

25. Xu R, Wang J, Kanezashi M, *et al.*: **Development of robust organosilica membranes for Reverse Osmosis.** *Langmuir.* 2011; **27**(23): 13996–13999.
PubMed Abstract | Publisher Full Text

26. Agirre I, Arias PL, Castricum HL, *et al.*: **Hybrid organosilica membranes and processes: status and outlook.** *Sep Purif Technol.* 2014; **121**: 2–12.
Publisher Full Text

27. Rimsza JM, Deng L, Du J: **Molecular dynamics simulations of nanoporous organosilicate glasses using Reactive Force Field (ReaxFF)**. *J Non-Cryst Solids.* 2016; **431**: 103–111.
Publisher Full Text

28. Chua YT, Lin CXC, Kleitz F, *et al.*: **Nanoporous organosilica membrane for water desalination.** *Chem Commun (Camb).* 2013; **49**(40): 4534–6.
PubMed Abstract | Publisher Full Text

29. Ayral A: **Sol-gel synthesis and fine characterization of hierarchically porous and multifunctional silica-based membranes.** *Chem Rec.* 2018; **18**(7–8): 878–890.
PubMed Abstract | Publisher Full Text

30. Abraham MJ, Murtola T, Schulz R, *et al.*: **GROMACS: high performance molecular simulations through multi-level parallelism from laptops to supercomputers.** *SoftwareX.* 2015; **1–2**: 19–25.
Publisher Full Text

31. See Supplemental Material at **10.5281/zenodo.14754876** which includes figures S1–S11, details on contact angle measurements, interface thickness measurement, hydrogen bond analysis, and ethanol carbon-carbon analysis.

32. Shi B, Dhir VK: **Molecular dynamics simulation of the contact angle of liquids on solid surfaces.** *J Chem Phys.* 2009; **130**(3): 034705.
PubMed Abstract | Publisher Full Text

33. Bussi G, Donadio D, Parrinello M: **Canonical sampling through velocity rescaling.** *J Chem Phys.* 2007; **126**(1): 014101.
PubMed Abstract | Publisher Full Text

34. Berendsen HJC, Postma JPM, Van Gun-steren WF, *et al.*: **Molecular dynamics with coupling to an external bath.** *J Chem Phys.* 1984; **81**(8): 3684–3690.
Publisher Full Text

35. Fuentes-Azcatl R, Alejandre J: **Non-polarizable force field of water based on the dielectric constant: TIP4P/ε.** *J Phys Chem B.* 2014; **118**(5): 1263–1272.
PubMed Abstract | Publisher Full Text

36. Jorgensen WL, Maxwell DS, Tirado-Rives J: **Development and testing of the OPLS all-atom force field on conformational energetics and properties of organic liquids.** *J Am Chem Soc.* 1996; **118**(45): 11225–11236.
Publisher Full Text

37. Emami FS, Puddu V, Berry RJ, *et al.*: **Force field and a surface model database for silica to simulate interfacial properties in atomic resolution.** *Chem Mater.* 2014; **26**(8): 2647–2658.
Publisher Full Text

38. Reif MM, Hünenberger PH, Oostenbrink C: **New interaction parameters for charged amino acid side chains in the GROMOS force field.** *J Chem Theory Comput.* 2012; **8**(10): 3705–3723.
PubMed Abstract | Publisher Full Text

39. Gravelle S: **simongravelle/publication-data: 31Mar2025**. 2025.
http://www.doi.org/10.5281/zenodo.15112114

40. **MAICoS: Molecular Analysis for Interfacial and Confined Systems**. Accessed: 2024–10–30.
Reference Source

41. Pártay LB, Hantal G, Jedlovszky P, *et al.*: **A new method for determining the interfacial molecules and characterizing the surface roughness in computer simulations. Application to the liquid–vapor interface of water.** *J Comput Chem.* 2008; **29**(6): 945–956.
PubMed Abstract | Publisher Full Text

42. Sega M, Hantal G, Fábián B, *et al.*: **Pytim: a python package for the interfacial analysis of molecular simulations.** *J Comput Chem.* 2018; **39**(25): 2118–2125.
PubMed Abstract | Publisher Full Text | Free Full Text

43. Michaud-Agrawal N, Denning EJ, Woolf TB, *et al.*: **MDAnalysis: a toolkit for the analysis of molecular dynamics simulations.** *J Comput Chem.* 2011; **32**(10): 2319–2327.
PubMed Abstract | Publisher Full Text | Free Full Text

44. MijakovićM, Polok KD, Kežić B, *et al.*: **A comparison of force fields for ethanol–water mixtures.** *Mol Simulat.* 2015; **41**(9): 699–712.
Publisher Full Text

45. Wakisaka A, Komatsu S, Usui Y: **Solute-solvent and solvent-solvent interactions evaluated through clusters isolated from solutions: preferential solvation in water-alcohol mixtures.** *J Mol Liq.* 2001; **90**(1–3): 175–184.
Publisher Full Text

Open Peer Review

Current Peer Review Status: ? ?

Version 1

Reviewer Report 03 October 2025

https://doi.org/10.21956/openreseurope.21108.r60182

© **2025 Breynaert E.** This is an open access peer review report distributed under the terms of the Creative Commons Attribution License, which permits unrestricted use, distribution, and reproduction in any medium, provided the original work is properly cited.

?

Eric Breynaert
NMRCoRe—NMR/X-Ray Platform for Convergence Research, Heverlee, Belgium

In their manuscript Gravelle and Coasne model the adsorption of water and ethanol from ethanol-water mixtures at organosilica and graphene interphases. The organosilica interphase compostion was varied from purely hydroxylated to (hydrophyllic) to purely methylated (hydrophobic). The study appears to be solid, but lacks to generate new insights and omits to link to existing literature on for example water organisation at organic and other confining interphases (e.g micelles, nanopores, etc.) for which it has been established that the number and length of the hydrogen bonds is reduced, which in turn affects NMR spectra, dielectric properties of such nanoconfined water phases.. In essence what the study models in the micropore of a membrane is closely related to the partitioning which forms the basis for many HPLC separations, but again no links are made towards scientific literature that field. In this respect it is peculiar the abstract mentions 'abnormal properties' since the observations described in the manuscript are exploited allready for decades in separation science. It would be interesting if the authors could link their molecular level observations, i.e. the described enrichment factor to macroscopic observations. Overall the present version of the manuscript appears to be more a report on methodology validation than that it provides exciting new results and insights.

Major Comment:
Data is provide at Zenodo with a link 'https://doi.org/10.5281/zenodo.14961713' which points to a zip file containing many data sets for many different publications. This makes it difficult to find the datasets pertaining to the present study and should be changed. The idea behind assigning doi's to datasets is to generate a direct link between a specific dataset and a manuscript.

Minor comment:
In the pdf version, page 3, paragraph 3: alcools is not English.

Is the work clearly and accurately presented and does it cite the current literature?
Partly

Is the study design appropriate and does the work have academic merit?

Partly

Are sufficient details of methods and analysis provided to allow replication by others?
Yes

If applicable, is the statistical analysis and its interpretation appropriate?
Not applicable

Are all the source data underlying the results available to ensure full reproducibility?
No

Are the conclusions drawn adequately supported by the results?
Yes

Competing Interests: No competing interests were disclosed.

Reviewer Expertise: molecular water science, physicochemical characterization, materials science

I confirm that I have read this submission and believe that I have an appropriate level of expertise to confirm that it is of an acceptable scientific standard, however I have significant reservations, as outlined above.

Reviewer Report 28 August 2025

https://doi.org/10.21956/openreseurope.21108.r55368

© 2025 Ghoufi A. This is an open access peer review report distributed under the terms of the Creative Commons Attribution License, which permits unrestricted use, distribution, and reproduction in any medium, provided the original work is properly cited.

?

Aziz Ghoufi
Paris-East Créteil University, Créteil, France

The work carried out by S. Gravelle and B. Coasne is rigorous, and the comparative study between different confinement states is relevant. The study focuses on the density profiles along the direction normal to the solid–liquid interface in order to capture the interfacial enhancement of density (for water or ethanol) as a function of surface chemistry.
The main result concerns surface enrichment in ethanol. While this is a predictable outcome, I understand that it still needs to be demonstrated explicitly.
Furthermore, similar results and discussions are already well documented in the literature (e.g., *Local Microphase Separation of a Binary Liquid under Nanoscale Confinement*, Morineau et al.).
Therefore, I do not clearly see the added value of this numerical work.
In my opinion, the more significant point would be to characterize the ethanol–water mixture structure—whether it forms hydrates or micelles—and the impact of the solid surface on these formations and their lifetimes.
Overall, this work appears rather trivial and simple, and it seems more like a preliminary study

than a complete investigation.
Formally, the work is technically sound and not incorrect, but I have doubts about the relevance and novelty of the results.

Is the work clearly and accurately presented and does it cite the current literature?
Yes

Is the study design appropriate and does the work have academic merit?
Partly

Are sufficient details of methods and analysis provided to allow replication by others?
Yes

If applicable, is the statistical analysis and its interpretation appropriate?
Yes

Are all the source data underlying the results available to ensure full reproducibility?
Yes

Are the conclusions drawn adequately supported by the results?
Yes

Competing Interests: No competing interests were disclosed.

Reviewer Expertise: nanoconfinement, interfacial properties, adsorption, molecular simulations

I confirm that I have read this submission and believe that I have an appropriate level of expertise to confirm that it is of an acceptable scientific standard, however I have significant reservations, as outlined above.